BEHAVIOUR OF GEOSYNTHETIC REINFORCED SOIL OVERLYING LOOSE SAND

Mohamed K. Hussein* Rami M. El-Sherbiny Mohamed I. Amer*****

ABSTRACT

This paper presents the results of experimental model tests to investigate the performance of geogrid as reinforcement element using strip footing model resting on geogrid reinforced replacement granular soil overlying loose sand. The model tests are conducted in a 1250 mm long, 400 mm wide, and 800 mm deep steel tank. A strip footing is simulated using a 30 mm thick, 100 mm wide, and 380 mm long steel plate. The purpose of the testing program is to determine the enhancement of ultimate bearing capacity of reinforced replacement soil, investigate the behavior of the generated strains at geogrid for different configuration of reinforced replacement soil, and to assess available methods for calculating the improved bearing capacity. The generated strains increase instantaneously by increasing the applied footing pressure. However, the rate of increasing the strains is low at lower settlement due to geogrid slack, and the rate increased at moderate settlement. The developed strains decreased gradually beyond the footing width due to occurrence pullout for reinforcement layers. Available analytical methods for calculating the improved bearing capacity are compared.

1- INTRODUCTION

The use of shallow foundations may be limited in many conditions due to excessive settlement and /or bearing capacity concerns resulting from the underlying soil. A reinforced soil foundation may enhance the performance of shallow foundations to acceptable limits. This involves replacing the existing weak soil up to a shallow depth with a compacted granular soil with inclusions of geogrid reinforcement layers to improve the ultimate bearing capacity and decrease settlements.

Few experimental studies were performed to investigate the bearing capacity of reinforced granular material underlain by soft clay [8, 10, 13, 15, 16, and 17]. Experimental study was performed using strip foundation resting on dense sand layer overlying soft clay reinforced with a layer of geogrid at the sand/clay interface [10].

*Teaching Assistant, Faculty of Engineering, Cairo University, Egypt. mohamed.kamal88@hotmail.com
**Associate Professor, Faculty of Engineering, Cairo University, Egypt. rsherbiny@eng.cu.edu.eg
***Prof. Dr., Faculty of Engineering, Cairo University, Egypt. mi.amer@ymail.com
Partial Fulfillment of the Requirements for the Degree of Doctor of Philosophy

They concluded that the optimum length of geogrid was 6B and the maximum benefit of the bearing capacity ratio was achieved by inclusion of a layer at the sand/clay interface where the depth ratio (H/B) equal 0.67. The optimum width of the reinforcement was 5B for strip footing and 3B for rectangular footings and the optimum number of layers was three which resulted in an increasing in bearing capacity by 45% and reduction in settlement by 15.7% [17].

Limited research is available on the bearing capacity of reinforced layered sand [9, 11, and 12]. Experimental investigation was executed to study the bearing capacity of reinforced layered sand using strip footings with thickness of top dense layer varies from 0 to 2B [11]. The ultimate bearing capacity increased up to 4 times the unreinforced case by inclusions of reinforcement layers up to 4 and the bearing capacity at settlement level (s/B) of 2% increased up to 3 times of unreinforced case [11]. However, the effect of using reinforcement layer has a minimal effect on the bearing capacity ratio at lower settlement value due to mobilizing membrane effect.

The present study investigates the enhancement of ultimate bearing capacity, the behavior of generated strains at geogrid for different configuration of reinforced soil, and to evaluate available methods for calculating the improved bearing capacity for a strip footing resting on geogrid reinforced replacement soil overlying loose sand with varying the number of geogrid layers and geogrid length.

2- TEST CONFIGURATION

2-1- Materials Properties

The tested soil used in this study is poorly graded sand. Grain size distribution was established according to ASTM D6913 [3]. Firstly the soil was passed through a sieve No.4 (4.75mm) to separate the coarse particles. The grain size distribution curve was illustrated in Figure (1). The soil is classified as poorly graded sand (SP) according to the unified soil classification system [1]. The angle of shearing resistance was determined using consolidated-drained triaxial tests [4] on samples prepared at relative densities of 36% and 78%, that represent the relative densities used in the physical model. The measured soil properties are summarized in Table (1).

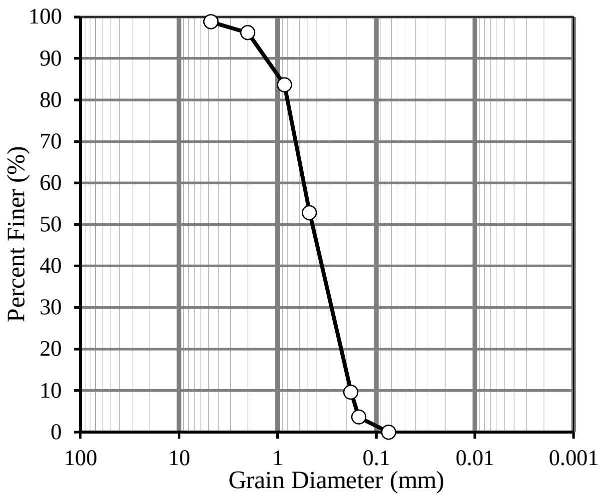

Figure 1- Grain size distribution of used sand. Source: Researcher

Table 1- Properties of sand material.

Soil Property	Value
Maximum dry unit weight (kN/m^3)	18.30
Specific gravity	2.65
Maximum void ratio	0.87
Minimum void ratio	0.43
Shearing resistance of dense sand ϕ (deg.)	42
Modulus of dense sand at σ'_3=50kPa, E_{50} (kPa)	10000
Shearing resistance of loose sand ϕ (deg.)	31
Modulus of dense sand at σ'_3=50kPa, E_{50} (kPa)	2000

2-2- Geogrid Properties

A commercially available biaxial geogrid, made from Polyethylene Terephthalate (PET) of the polyester group of polymers is commonly used as a fiber or in strips of geotextile and geogrid products. PET is less susceptible to oxidation, creep, and stress cracking. Some properties of geogrid that was used as reinforcement element as illustrated in Table (2). The geogrid properties were obtained from standard test method to determine tensile properties of geogrids according to ASTM D 6637 –01[2]. The tests were conducted in the Geosynthetic lab of Construction Research Institute (CRI) in Cairo. Fig. (2) shows the initial installation of geogrid Testometric machine where the sample width was 200 mm, the sample height was 300 mm, and the test speed was 20 mm/min. Series of tests were conducted to ensure repeatability of the test results to determine the stress strain curve as illustrated in Fig. (3). Two strain gauges were installed at the mid and the upper third height of geogrid specimen to estimate the relation between global strain and local strain, therefore the measured strain at physical model can be converted to global strain using Figure (4).

Table 2- Properties of geogrid material

Geogrid Property	Value
Ultimate tensile strength (kN/m)	15
Strain at ult. tensile strength (%)	18
Secant stiffness @strain 2% (kN/m)	160
Secant stiffness @strain 5% (kN/m)	105
Opening size (mm)	3.5

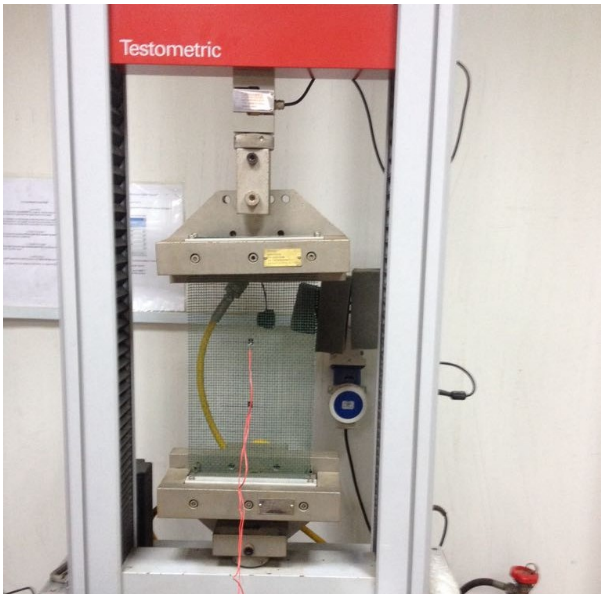

Figure 2- Installation geogrid at Testometric machine to determine tensile properties. Source: Researcher

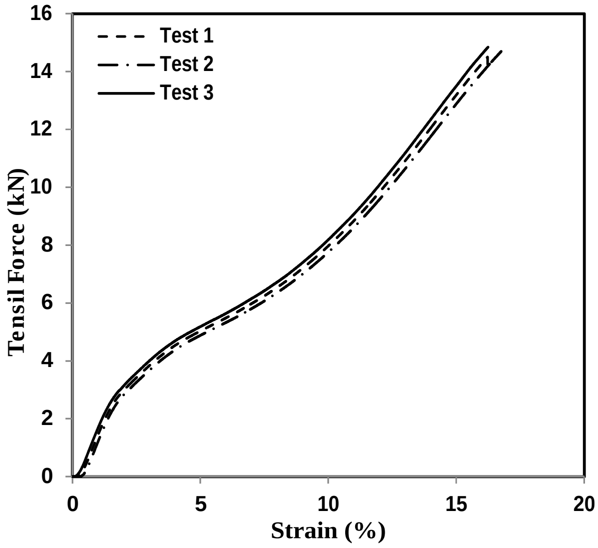

Figure 3. Tensile force versus strain for tested geogrid. Source: Researcher

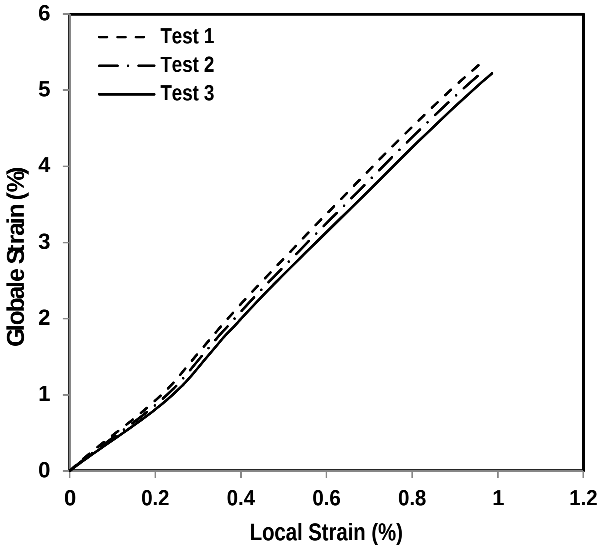

Figure 4. Global strain versus local strain for tested geogrid. Source: Researcher

2-3- Test Device

The model tests were conducted in a 1250 mm long, 400 mm wide, and 800 mm deep steel tank. The tank was fabricated from 5 mm thick steel sheet. One side of the tank was fabricated from 10 mm thick acrylic sheet. The tank was braced with structural steel members to avoid lateral deformation during loading. The model footing used in the tests is 30 mm thick steel plate with dimensions of 100 mm x380 mm (BxL) for strip footings. A small groove was made at the centre of the model footing to ensure that the applied load is at the centre for uniform distribution of the vertical load. The loading frame consists of 6.0 m long horizontal steel beam connected with two vertical steel beam that enable the horizontal beam to rotate around the point of connection. To make the beam horizontal, a 2.5 kN was applied at the end of the beam to equivalent own weight of the beam. The beam was loaded incrementally at the end bracket and the load was applied to the plate using vertical loading rod connected with the beam by hinge connection to prevent the loading rod from rotation and remain vertical during loading as illustrate in Fig. (5). An axial load was applied in increments of 50 N with lever arm ratio of 10 that results a force of 500 N and a stress of 13.2 kN/m^2 to the model footing. An axial load was increased after the footing settlement was finished. A MTS 661.19 Force Transducer of 25 kN capacity was used to monitor the load increments. The footing settlement was measured using two linear voltage displacement transducer (LVDT) that located at the footing edge. All data was transferred using DATA PLATFORM GL7000

Figure 5- Arrangement of the test device. Source: Researcher

2-4- Test Procedure

At first the sand was placed inside the tank using a funnel and controls the soil to fall by gravity up to a depth of 600 mm, and then the surface of the sand was levelled. The amount of sand was predetermined to achieve the required relative density of 36% for loose state.

After Preparation of loose sand, the amount of sand for one layer of 30 mm thick was poured into the tank to achieve the target relative density of 76% for dense state that representing 0.95 of maximum dry unit weight obtained from modified proctor test, then the surface of the sand layer was levelled at the loose state and compacted using a 10 mm x 38 mm wooden plate and hand rammer to achieve the predetermined height of 30 mm. The same procedure was repeated to prepare the upper layer till achieving the total thickness of dense layer. It is important to mention that, using the hand rammer shall be strict to prevent the loose sand from subjecting to compaction effort and the number of blows required to achieve the target relative density shall be increased to decrease the compaction effort, then the effective depth during compaction decreased.

For reinforced layer, the reinforcement was centred underneath footing centre, and then the sand was filled at the centre of geogrid layer to ensure the geogrid was stretched during levelling the sand. For each test, the tank was fully emptied and replaced with sand using the same procedure to obtain the desired densities and reinforcement configurations to ensure standardised conditions during the study.

2-5-Testing Program

A series of tests was conducted to determine the enhancement of ultimate bearing capacity, study the behavior of generated strains at geogrid for different configuration of reinforced soil, and to evaluate available methods for calculating the improved bearing capacity.The testing program was organized to study the effect of the number of reinforcement layers (N = 1, 2, 3) and length of reinforcement (L = 6B, 4B, 2B) on improvement of ultimate bearing capacity. All tests were performed at constant spacing between layers (h), first layer spacing from footing base (u), and thickness of dense layer (d). Some of tests were repeated at least two times to ensure repeatability of the test results. Table (3) summarizes the testing program. Each test is identified using a string (d-N-L-u/B-h/B) representing the test configuration.

Table 3.Testing program.

Test No.	N	u/B	h/B	d/B	L/B
1	0	-	-	1.2	-
2-4	1	0.3	0.3	1.2	2,4,6
5-7	2	0.3	0.3	1.2	2,4,6
8-10	3	0.3	0.3	1.2	2,4,6

3- RESULTS AND ANALYSIS

A series of tests were performed on strip footing resting on geogrid reinforced granular soil overlying loose sand. The purpose of testing program was to investigate the enhancement of ultimate bearing capacity and study the behavior of generated strains at geogrid for different configuration of reinforced soil. The effect of the number of reinforcement layers and reinforcement length were discussed below where the improvement of ultimate bearing capacity is calculated using Equation (1).

$BCR_u = q_{uR}/q$.. (1)

Where q_{uR} and q are the ultimate bearing capacity for the reinforced and unreinforced soil, respectively that were determined based on tangent intersection method [19].

3-1- Effect of Number of Reinforcement Layers

Typical stresses–settlement curves are illustrated in Figure (6). The tests were performed at different number of layers (N=1, 2, 3), the first layer spacing (u) of 30 mm, spacing between layers of 30 mm, and the thickness of dense layer of 120 mm. Failure modes of unreinforced and reinforced soil were observed a punching shear failure in the laboratory tests. It was observed that occurrence punching shear failure for reinforced soil with one layer of geogrid located at depth of 30 mm below the base of footing. With increasing the number of geogrid layer, the ultimate bearing capacity ratio increased as illustrated in Figure 7. As the soil under the footing settled downward, the reinforcement layer deformed and tensioned that develops an upward force component supporting the external applied loads. This phenomenon called membrane effect that reduced occurrence of soil punching and distribute the stresses on a large area beneath the footing. However, mobilizing membrane effect required some settlement and development of tension in the reinforcement resulting from interlocking and friction between the soil and geogrid. Figure (7) shows that the ultimate bearing capacity ratio increased by 10%, 46%, and 59% when increasing the number of reinforcement layers by one, two, three layers having a width of 6B respectively. It is noted that, the number of geogrid layers has a minimal effect on the bearing capacity ratio at lower settlement value due to mobilizing membrane effect.

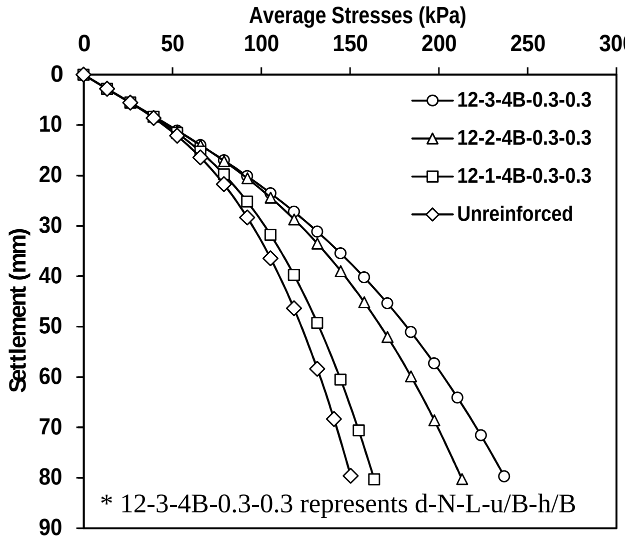

Figure 6- Stresses versus settlement curves for d =1.2B.
Source: Researcher

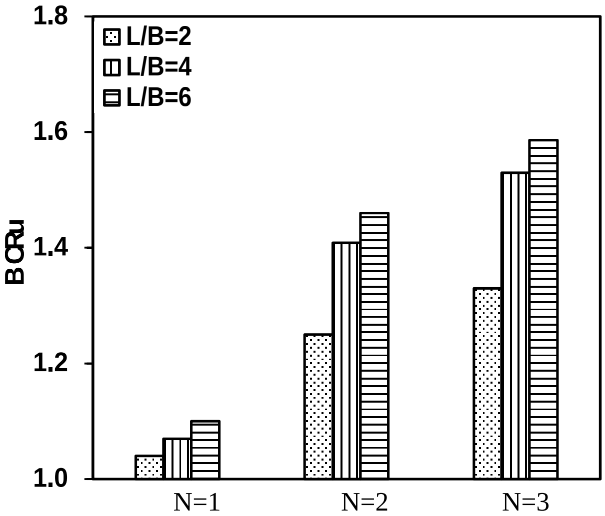

Figure 7- Ultimate bearing capacity ratio versus number of layers
Source: Researcher

3-2- Effect of Reinforcement Width

Fig. (8) shows that the ultimate bearing capacity ratio increased with increasing geogrid length; the BCRu for reinforced soil using three layer improved by 33%, 53%, and 59%for geogrid length of 2B, 4B, and 6B respectively. For two layers of geogrid, the BCRu increased by 25%, 41%, and 46%for geogrid length of 2B, 4B, and 6B, respecttively. It is noted that the improvement of geogrid length have a minimal effect beyond 4B. The improvement resulting from increasing the reinforcement length was due to increasing geogrid anchorage length that increased the pullout resistance. The effect of geogrid length for reinforced soil by one layer having first layer spacing of 30 mm below the footing base was insignificant due to inadequacy of applied effective stresses on the anchorage length; therefore pull out resistance increased insignificantly as the geogrid extent increased.

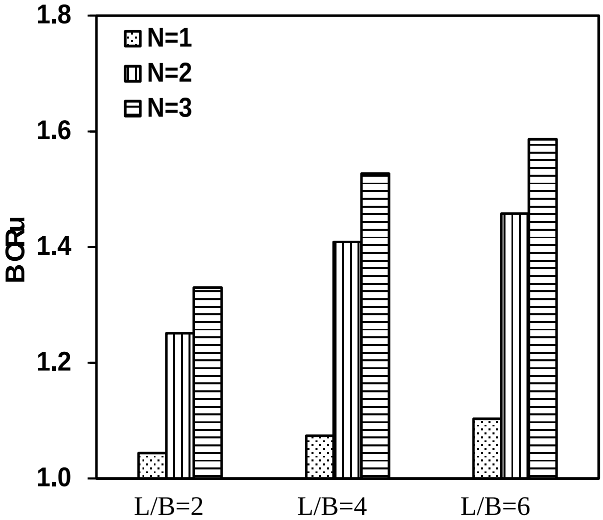

Figure 8- Ultimate capacity ratio versus reinforcement length.
Source: Researcher

3-3- Strain Distribution along Reinforcement

Strain gauges were installed at different locations along the reinforcement to measure the generated strains; therefore the tensile force can be calculated. The strain gauges installed at a distance measured from the centerline of the footing to the reinforcement length (x/L). The values of (x/L) were 0, 0.25, and 0.4 except the case of reinforcement length of 2B; the values of (x/L) were 0 and 0.38. Fig. (9) shows the generated stains versus settlement for different locations where the generated strains increased instantaneously by increasing the applied footing pressure. However, the rate of increasing the strains was low at lower settlement due to geogrid slack, and the rate increased at moderate settlement. On the other hand, at higher settlement the rate of increasing the strains becomes minimal due to occurrence of geogrid pullout. Fig. (10) shows the generated stains versus distance ratio measured from the center line of the footing. The generated stains increased instantaneously by increasing footing pressure, therefore the drawn strains in Fig. (10) were observed at the ultimate bearing capacity. It can be noted, the developed strains decreased gradually beyond the footing width due to occurrence pullout for reinforcement layers. The strains increased by increasing the reinforcement length and the layer depth due to increasing the overburden pressure applied on the geogrid that enhanced the pullout resistance resulting from interlocking and friction between the soil and geogrid.

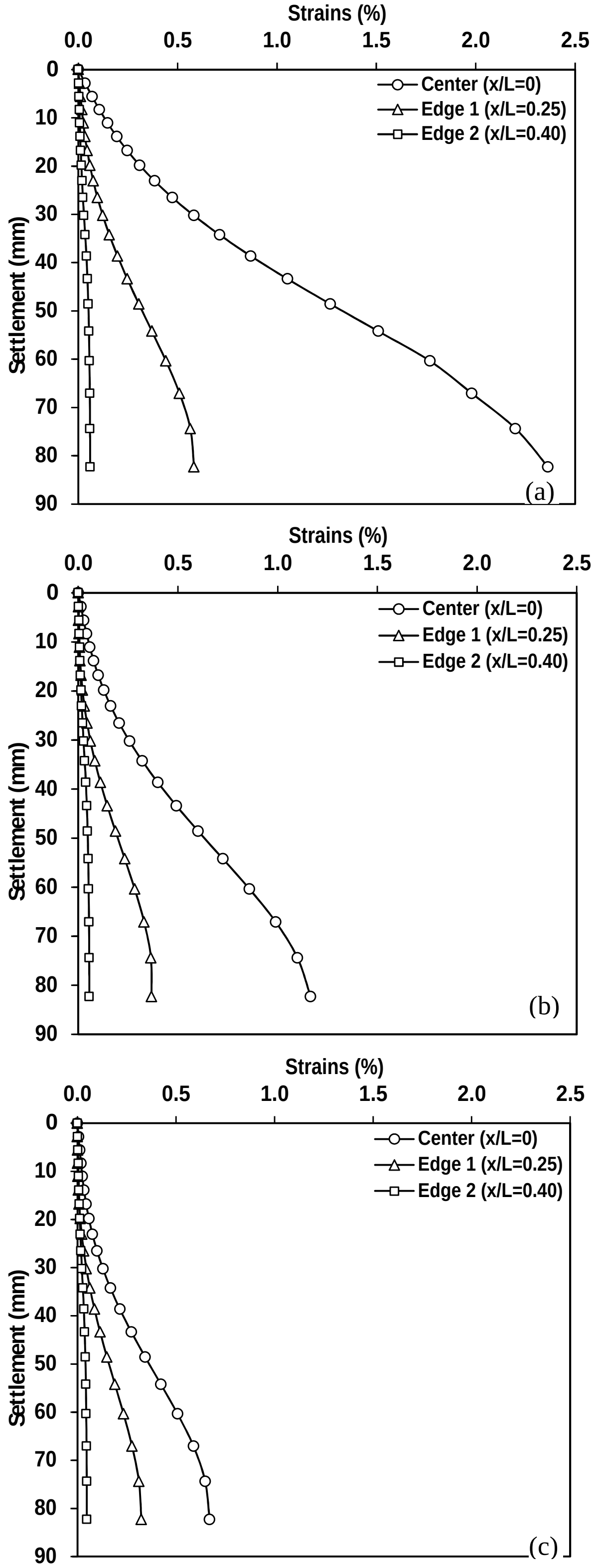

Fig. 9- Strains versus settlement curves for different locations For N=3 and L=6B (12-3-6B-0.3-0.3): (a) Third layer, (b) second layer, (c) first layer. Source: Researcher

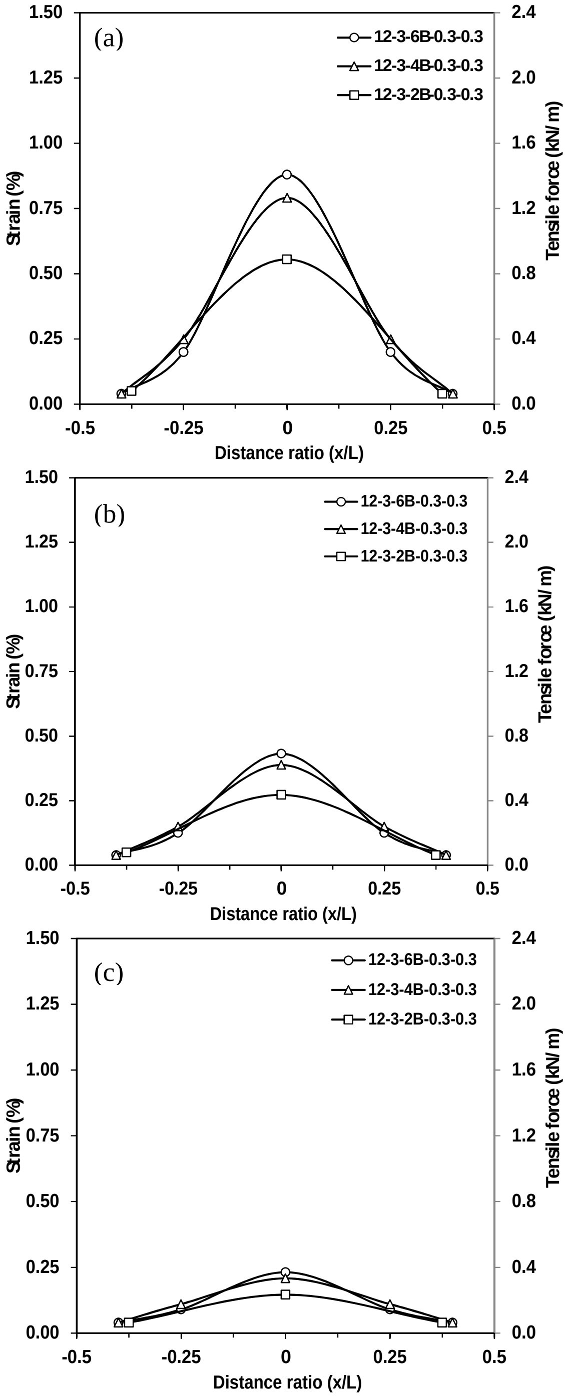

Fig. 10- Strain distribution along reinforcement with various width and N= 3. (a) Third layer, (b) second layer, (c) first layer. Source: Researcher

4- COMPARISONS BETWEEN TEST RESULTS AND ANALYTICAL SOLUTIONS

Wayne et al., 1998 [20] proposed analytical method to calculate the ultimate bearing capacity of two layer system including the contribution of reinforcements. They modify Meyerhof and Hanna's (1978) equation [14] for dense soil overlying weak soil to incorporate reinforcement effect of strip footing resting on reinforced soil as shown in Equation 2 that represent punching shear failure through the reinforced zone followed by general shear failure.

$$q_{uR} = q_{un} + \frac{2C_a d}{B} + \gamma d^2 (1+\frac{2df}{d}\frac{K_s \varphi}{B} + \gamma d + \Sigma_{i=1}^{N}\frac{(2T)}{B} \quad \text{.....(2)}$$

(2)where c_a is adhesion of reinforced soil; γ is the unit weight of soil in reinforced zone; D_f is the embedment depth of the footing; K_s is the punching shear coefficient, which depends on the angle of internal friction for reinforced soil and the ratio between the ultimate bearing capacity of dense soil and weak soil; and T is the tensile force in reinforcement determined using strain gauges measurements and tensile modulus of reinforcement.

Sharma et al., (2009) [18] suggest analytical method to calculate the ultimate bearing capacity of reinforced soil based on the limit equilibrium analysis proposed the failure occur within reinforced zone. The ultimate bearing capacity of strip footing increased due to the tensile force developped in the reinforcement (Δq_t) as shown in Equation (3). Chen and Abu-Farsakh (2015) [7] developed an analytical solution to estimate the ultimate bearing capacity of reinforced soil. They proposed a failure mechanism that considers both the confinement and the membrane effects as shown in Equation (4).

$$\Delta q_t = \sum_{i=1}^{N} (\frac{4T(u+i-1)h}{B^2}) \quad \text{.................(3)}$$

$$\Delta q_u = \sum_{i=1}^{N} \frac{2T\cos\alpha\tan\delta + 2T\sin\alpha}{B} \quad \text{......(4)}$$

Where δ is the mobilized friction angle along punching surfaces which equal angle of shearing resistance of upper soil; α is the angle of tensile force with the horizontal which assumed as 5 and 20° [7].

Figure (11) shows comparison between the (BCR_u) obtained from the experimental test results and the analytical methods by applying the measured tensile forces. It can be noted that Chen and Abu-Farsakh (2015)'s method using angle of tensile force with the horizontal of 20^0 resulted in a better prediction of BCR_u due to consideration of both the confinement and the membrane effects where the BCRu obtained has a good agreement with model results with a maximum error of less than 5%. Wayne et al. (1998) and Chen and Abu-Farsakh (2015)'s method using angle of tensile force with the horizontal of 5^0 provided underestimated BCR_u values. On the other hand, Sharma et al. (2009)'s method provided overestimated with error up to 33%.

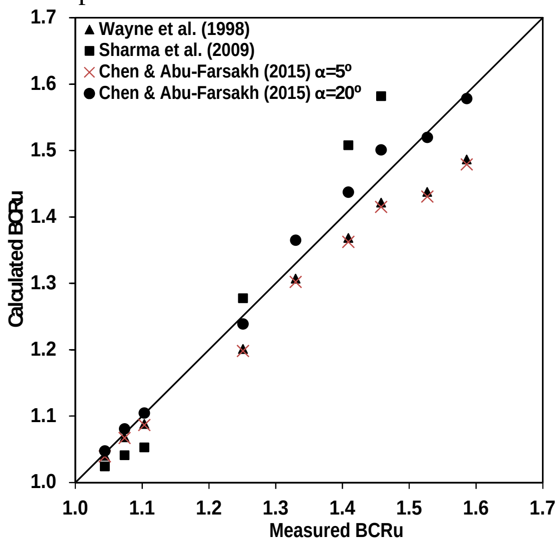

Figure 11- Comparison of the experimental results and estimated BCRu analytical methods. Source: Researcher

5- CONCLUSIONS

Series of physical model tests were performed to study the behaviour of strip footing resting on geogrid reinforced replacement soil overlying loose sand to investigate the enhancement of the ultimate bearing capacity and study the behavior of generated strains at geogrid. The test results show the following conclusions:

1- The maximum benefit of using geogrid reinforced soil is achieved at reinforcement length of six times footing width and number of reinforcement layers of three.

2- The generated strains increased instantaneous by increasing the applied footing pressure. However, the rate of increasing the strains was low at lower settlement due to geogrid slack, and the rate increased at moderate settlement.

3- The generated strains at geogrid reinforcement were decreased gradually beyond the footing width.

4- The strains generated at the deep layer were more efficient than the shallow layer.

5- Chen and Abu-Farsakh (2015)'s method resulted in a better prediction of BCR_u due to consideration of both the confinement and the membrane effects.

REFERENCES

1- ASTM D2487 - Standard Practice for Classification of Soils for Engineering Purposes (Unified Soil Classification System), ASTM International.

2- ASTM D6637-01 - Standard Test method for determining tensile properties of geogrids, ASTM International.

3- ASTM D6913 Standard Test Methods for Particle-Size Distribution (Gradation) of Soils Using Sieve Analysis, ASTM International.

4- ASTM D7181 Method for Consolidated Drained Triaxial Compression Test for Soils, ASTM International.

5- Binquet, J. and Lee, K.L. (1975). Bearing capacity analysis on reinforced earth slabs, Journal of Geotechnical Engineering Division, ASCE 101 (GT12), pp. 1257–1276.

6- Cerato, B.A. (2005). Scale effects of shallow foundation bearing capacity on granular material, PhD thesis of Massachusetts Amherst University, USA.

7- Chen, Q., Abu-Farsakh, M. (2015). Ultimate bearing capacity analysis of strip footings on reinforcedsoil foundation. Soils and Foundations, http://dx.doi.org/10.1016/j.sandf.2014.12.006.

8- Consoli, N.C., Rosa, F.D., and Fonini, A. (2009). Plate load tests on compacted soil layers overlying weaker soil, J. of Geotechnical. &Geoenvironmental Engineering, ASCE, 135 (12), pp. 1846-1856.

9- Elvidge B.C. (1999). Effect of reinforcement length on the bearing capacity of footings on shallow granular layers, Master degree thesis, University Queen, Ontario, Canada.

10- King, K.H., Das, B.M., Puri, V.K., Yen, S.C., and Cook, E.E. (1993). Strip foundation on sand underlain by soft clay with geogrid reinforcement, Proceedings of the third (1993) International Offshore and Polar Engineering Conference, Singapore (1), pp. 517-521.

11- Kumar. A, Ohri M. L., and Bansal R. K. (2007). Bearing capacity tests of strip footings on reinforced layered soil, Geotechnical and Geological Engineering, 25, pp.139–150

12- Kumar.A. and Walia B.S. (2006). Bearing capacity of square footings on reinforced layered soil, Geotechnical and Geological Engineering, 24, pp. 1001–1008.

13- Love, J.P., Burd. H.J., Milligan, G.W.E., and Houlsby, G.T. (1987). Analytical and model studies of reinforcement of a layer of granular fill on a soft clay subgrade, Canadian Geotechnical Journal, 24(4), pp. 611-622.

14- Meyerhof, G.G. and Hanna, A.M. (1978). Ultimate bearing capacity of foundations on layered soils under inclined load. Canadian Geotechnical Journal, 15 (4), pp. 565–572.

15- Mohamed, M.A. (2010). Two dimensional experimental study for the behaviour of surface footing on unreinforced and reinforced sand beds overlying soft pockets, Geotextiles and Geomembranes, 28, pp. 589-596.

16- Ornek, M. (2009). Geogrid reinforcement on soft clay deposits, PhD Dissertation, University of Cukurova, Turkey.

17- Rethaliya, R.P. and Verma, A.K. (2009). Footings on sand overlying soft clay with geosynthetics interface, PhD Dissertation, Sardar Patel University, India.

18- Sharma, R., Chen, Q., Abu-Farsakh, M., and Yoon, S. (2009). Analytical odelling of reinforced soil foundation, Geotextiles and Geomembranes, 27 (1), pp. 63–72.

19- Trautmann, C.H., and Kulhawy, F.H. (1988). Uplift load-displacement ehaviour of spread foundations, Journal of Geotechnical Engineering, ASCE, 114 (2), 168-183.

20- Wayne, M.H., Han, J., and Akins, K. (1998). The design of geosynthetic reinforced foundations, In: Proceedings of ASCE’s 1998 Annual Convention & Exposition. ASCE Geotechnical Special Publication 76, pp. 1–18.